



HAL
open science

Hydrometeorological Extreme Events in Africa: The Role of Satellite Observations for Monitoring Pluvial and Fluvial Flood Risk

Marielle Gosset, Pauline Dibi-Anoh, Guy Schumann, Renaud Hostache, Adrien Paris, Eric-Pascal Zahiri, Modeste Kacou, Laetitia Gal

► **To cite this version:**

Marielle Gosset, Pauline Dibi-Anoh, Guy Schumann, Renaud Hostache, Adrien Paris, et al.. Hydrometeorological Extreme Events in Africa: The Role of Satellite Observations for Monitoring Pluvial and Fluvial Flood Risk. *Surveys in Geophysics*, 2023, 44 (1), pp.197-223. 10.1007/s10712-022-09749-6 . hal-04379950

HAL Id: hal-04379950

<https://hal.science/hal-04379950>

Submitted on 18 Jan 2024

HAL is a multi-disciplinary open access archive for the deposit and dissemination of scientific research documents, whether they are published or not. The documents may come from teaching and research institutions in France or abroad, or from public or private research centers.

L'archive ouverte pluridisciplinaire **HAL**, est destinée au dépôt et à la diffusion de documents scientifiques de niveau recherche, publiés ou non, émanant des établissements d'enseignement et de recherche français ou étrangers, des laboratoires publics ou privés.



Hydrometeorological Extreme Events in Africa: The Role of Satellite Observations for Monitoring Pluvial and Fluvial Flood Risk

Marielle Gosset¹ · Pauline A Dibi-Anoh² · Guy Schumann^{3,4} · Renaud Hostache^{5,6} · Adrien Paris^{7,8} · Eric-Pascal Zahiri² · Modeste Kacou² · Laetitia Gal^{7,8}

Received: 2 February 2022 / Accepted: 23 October 2022 / Published online: 10 January 2023
© The Author(s) 2023

Abstract

This article reviews the state of the art in the use of space-borne observations for analyzing extreme rainfall and flood events in Africa. Floods occur across many space and timescales, from very localized flash flood events to slow propagation of discharge peaks in large rivers. We discuss here how satellite data can help us understand the genesis and impacts of these flood events, monitor their evolution, and better constrain prediction models, thereby improving early warning and population protection. To illustrate these topics, we reanalyze major flood events that occurred in Niger, Mozambique, Central African Republic and Ivory Coast, using satellite information.

Keywords Remote sensing · Flood · Climate change · Extremes · Early warning systems · Satellite monitoring

✉ Guy Schumann
Guy.Schumann@bristol.ac.uk

Marielle Gosset
Marielle.gosset@ird.fr

¹ UMR GET (IRD/CNRS/Université Toulouse III/CNES), 14, Avenue Ed Belin, Toulouse, France

² University Félix Houphouët-Boigny (UFHB), 01 BP V34, Abidjan, Côte d'Ivoire

³ School of Geographical Sciences, University of Bristol, Queens Road, Bristol BS8 1SS, UK

⁴ Research and Education Department, RSS-Hydro, 100 Route de Volmerange, 3593 Dudelange, Luxembourg

⁵ Environmental Research and Innovation (ERIN) Department, Luxembourg Institute of Science and Technology (LIST), 41 Rue du Brill, 4422 Belvaux, Luxembourg

⁶ UMR Espace-Dev (IRD, Univ. Reunion, Univ. Guyane, Univ. Antilles, Univ. Nouvelle Calédonie, Univ. Montpellier), 500 Rue Jean François Breton, 34090 Montpellier, France

⁷ Hydro Matters, 1 Chemin de la Pousaraque, 31460 Le Faget, France

⁸ UMR LEGOS (Université de Toulouse/CNES/CNRS/IRD), 14, Avenue Ed Belin, 31400 Toulouse, France

Article Highlights

- Pluvial and fluvial floods are becoming more and more frequent in Africa under the combined effect of global warming and intense urbanization
- The casualties and material damages associated with extreme rainfall events and floods in Africa could be reduced with better monitoring and prediction of these phenomena, but the state of the in situ hydrometeorological networks is inadequate for such a surveillance
- Satellite observations can play a major role in complementing the in situ networks for the development of efficient flood early warning systems in Africa
- Major recent flood events in Africa have been well depicted by satellite observations, illustrating the feasibility of satellite monitoring for better surveillance of the flood risk in this region

1 Introduction

There is observational evidence that hydrometeorological extremes, droughts and floods, are increasing worldwide. As stated by the United Nations report “Reducing disaster risk” (UNDP/BCPR 2004) in the time period 1980–2000 around 196 million people in more than 90 countries were exposed on average every year to catastrophic flooding and 170,010 deaths were associated with floods. The World Bank (WorldBank 2021) reports that over the last two decades at least 1.65 billion people have been affected by floods and 1.43 billion by droughts, worldwide. In terms of risk, floods represent nearly half of the disasters that have occurred for the last 20 years according to the Center for Research on the Epidemiology of Disasters (CRED 2020). This number rises to more than 70% if storms (often linked with inundation events) are also included. These amounts have largely increased compared to 1980–1999 (CRED 2020). Floods are also the main reason for the activation of the Copernicus Emergency Management Service (EMS). Among the 418 activations of the Copernicus EMS over the period 2012–2020, about 50% of them are related to hydrometeorological events (*see EMS Copernicus*, activation inventory <https://emergency.copernicus.eu/mapping/list-of-activations-rapid>). These observations are consistent with the intensification of the hydrological cycle expected from global warming and a higher hydroclimatic intensity as defined by Giorgi et al. (2011) and reported in the Sixth Assessment Report of the Intergovernmental Panel on Climate Change (IPCC 2022). Using global and regional climate model experiments, these authors show that precipitation intensity and the length of dry periods should indeed increase in an interconnected fashion with increased temperatures. Panthou et al. (2018) used daily and sub-daily rain gauge records to quantify the evolution of rain intensities in Sahel over the last decades. They conclude that a hydroclimatic intensification is actually taking place, with a higher contribution of heavy rainfall to the annual rain totals. Similar conclusions were drawn by Trambly et al. (2020) for all of Africa, showing a consistent trend in the increase of floods and intense rainfalls over the last 3 decades. This evolution of flooding in Africa over the last decades is due to the combined effect of changes in the climatic forcing (interannual variability and global warming) and changes in the hydrological response of the basins. The latter is due to many factors, such as the construction of dams or land use and land cover changes. The replacement of natural vegetation by cultures and urbanization tends to decrease the infiltration capacity of the soils and increase runoff, accelerating the basins hydrological response.

Di Baldassarre et al. (2010) report that flood-related fatalities and associated economic losses have increased dramatically over the past half-century in Africa. In addition to the increase of flood occurrence, another cause of these increasing damages is the intensive and unplanned human settlements, in urban and rural flood-prone areas (Li et al. 2016; Tiepolo and Galligari 2021). The means of prevention and the capacity to respond in the event of a disaster are also less developed in southern regions like Africa than in most northern countries.

There is therefore a pressing need for an improved understanding and evaluation of flood hazard at global scale (UNISDR 2015). Data on river flow and estimates of flood hazard are still of insufficient quality in many regions of the world (Wright 2015; Haile et al. 2022), hampering the implementation of appropriate mitigation measures. The situation could be improved by means of satellite information.

Satellite observations are becoming (and already are, to some extent) an important contribution to the collective effort to improve flood risk reduction policies. Satellite observations have been useful to analyze trends in extreme events and other factors that influence floods (land use changes, for instance). They are used for mapping the flood-prone areas and derive vulnerability indicators. They contribute to real-time monitoring of extreme events and flood forecasting and provide guidance for emergency interventions.

Section 2 discusses the flood risk and the need to enhance hydrometeorological observations in Africa. Section 3 introduces satellite sensors and products of interest for flood analysis and prediction. Section 4 illustrates the use of satellite information on some concrete recent major flood events in Africa, including Mozambique, Niger, Central Africa Republic and Ivory coast, spanning a variety of flood processes and different spatial–temporal scales.

2 Flood Phenomena and Deficit of Hydrometeorological Observations in Africa

2.1 Flood Phenomena and Observational Needs

There are different physical processes that lead to floods. They result in a large range of flood types and scales. The spatial extension and duration of the flooding vary from very localized and short duration events to extended and long-lasting floods, both in rural or urban areas; the floods can be directly related to intense rainfall (pluvial origin) combined with lack of infiltration or/and due to the overflow of a river.

All types and scales of floods happen in Africa, as illustrated on a few case studies in Sect. 4, and the damages associated with these phenomena have dramatically increased in this region over the past half-century (Di Baldassarre et al. 2010; Trambly et al. 2020).

Floods put at-risk investments in infrastructure, agriculture, human health, water resources, disaster management, and the environment. For example, the transportation infrastructure in Africa is crucial to bringing Africa out of poverty, but flooding incapacitates large parts of this network every year. Weather extremes also increase the vulnerability of people—particularly the poorest. A key to reduce damages and improve resilience to these natural hazards, is to be able to monitor and forecast the evolutions of flood events. This is why reliable observations are needed, and preferably in real time. A few studies have tried to quantify the actual benefit of improving flood forecasts. Rogers and Tsirkunov (2010) report that damage reduction due to forecast improvements can range from a few

percentage points to as much as 35 percent of average annual flood damages. Hawley et al. (2022) compared several flood risk management approaches. They conclude that forecasting and early warning systems have a high benefit–cost ratio (second only to floodplain restoration and far greater than heavy infrastructure such as embankments, dams). Pappenberger et al. (2015) estimated the monetary benefits of flood early warning in Europe to be of the order of €400 for every €1 invested. These results confirm the need for quality hydrometeorological observations in order to survey these natural phenomena and their impacts, with observational time and spatial scales adequate to detect their onset and monitor their dynamics, in all continents.

In pluvial and small river flash floods, the trigger event is usually an intense rainfall event (or a close succession of events) generating runoff over an area with low infiltration capacity. The timing and spatial extension of these floods are closely related to those of the triggering rainfall event. This type of floods is common in catchments with high slopes, mountainous areas and deep valleys, and also in urbanized areas with impermeable soils. The small spatial scales and delays involved, make the observation and prediction of these phenomena a challenge. Unless in situ water-level gauges are present, the monitoring of such events is based on rainfall analysis. In industrialized countries, networks of weather radar are very useful, yet not perfect (Berne and Krajewski 2013) to detect localized and rapid flood risk.

Fluvial flooding can occur over a range of scales, from a few days to a few weeks and even months. The trigger is generally intense rainfall that saturates the soil of hydrological basins and generates flood waves that propagate along the drainage network and make rivers burst their banks. Several examples of fluvial flooding from major African rivers, involving propagation times of two days (Niger) to several weeks (Oubangui), are provided in Sect. 4. When the flood wave travel time is long enough, the risk of fluvial flooding downstream can be predicted by detecting the peak flow upstream and using statistical and/or hydrodynamical modeling.

The Niger river in Niamey offers interesting example of floods over different scales, with both the propagation of the slow peak flow coming from the upper Niger and a relatively fast response to local rainfall must be considered for prediction and monitoring the fluvial floods in Niamey. In that case, a hydrological model coupled with a hydrodynamical model is necessary (Fleischmann et al. 2018) together with rainfall estimation over the areas contributing to local runoff and information on river water levels upstream water (see Sect. 4.2).

2.2 Limitations of the Hydrometeorological Observation Networks in Africa

Unfortunately, the current hydrometeorological observation networks in Africa are not adequate to provide the density and quality of information needed to survey flood risk over this continent. International organizations like the World Meteorological Organization (WMO) or the World Bank (WB) have reported on the worrying state of National Meteorological and Hydrological Services (NMHSs) in poor countries and specially in Africa (Rogers and Tsirkunov 2013). They analyze how the situation of many NMHSs in developing and least developed countries has worsened over the last decades and the observation networks have deteriorated primarily because of underfunding and in some instances military conflict. They consider that substantial human and financial losses could have been prevented if meteorological and hydrological agencies had access to reliable observational and forecasting tools.

The scarcity of the in situ hydrological network in Africa and its degradation in recent times is discussed in Papa et al. (2023), in this issue. As an example, they report that the number of hydrological gauges in the Congo collapsed, from 400 operational stations by the end of 1960s, to 15 gauges considered as operational currently. Most African rivers suffer from a deficit of real-time in situ monitoring (Haile et al. 2022; Trambly et al. 2021), worsen by data sharing issues for transboundary basins.

The situation of the meteorological network is similarly worrying, and the contrast with industrialized countries is striking. For instance, the only country in sub-Saharan Africa where weather radar is operational and sufficiently quality controlled to be used for quantitative rainfall estimation in South Africa, with 12 radars. By contrast, there are over 200 operational weather radar in Europe—with 30, only in France. Even the network of daily rain gauges is extremely scarce in Africa (Kidd et al. 2017; Lorenz and Kunstmann 2012). Alternative solutions are being developed such as the Trans-African Hydro-Meteorological Observatory (TAHMO) project aiming to provide a dense network of low-cost stations in many African countries. Rainfall monitoring based on commercial microwave links from cellular phone network is also an interesting alternative for Africa (Turko et al. 2021; Gosset et al. 2016), but not yet fully operationalized or used by the NMHSs.

Satellite observations can contribute to filling the observational gaps in Africa and be used to develop flood monitoring tools. This is discussed in the next sections.

3 Satellite observations Relevant for Flood Analysis and Prediction

The use of satellite information in hydrology is growing. Papa et al. (2023) in this issue provide a rich overview of the techniques available for surveying surface waters from space, both in terms of their storage and fluxes. Their paper reviews recent progress using satellite observations over Africa for monitoring the water resource and its quality, and to characterize many hydrological processes.

In this section, we focus specifically on the satellite information potentially useful for operational flood monitoring—with a special interest for data available with short latency.

3.1 Storm Monitoring and Rainfall Estimation from Satellite

Rainfall is the primary driver of the continental hydrological cycle, and floods are mainly explained by an excess of rainfall over a certain area and time. The rainfed area and period are very localized in the case of flash floods and pluvial flooding, for which the trigger variable is the rainfall intensity. For larger-scale floods, rainfall accumulation over time and integrated over large areas are usually needed.

Meteorological satellites have brought a revolution in weather services worldwide by offering a global coverage (land and oceans) with high resolution and frequent sampling. This is true for geostationary satellites, such as the Meteosat series in Africa which provide information every 15 min and a few kilometers. However, these satellites, equipped with infra-red (IR) and visible channels, provide information on clouds rather than on the rain itself.

High-resolution information from geostationary satellites (Meteosat Second Generation or MSG in Africa) is available in real time and can be used to monitor the evolution and the severity of storms. The long (over 3 decades) available series of geostationary data has been used to document the typical life cycle of tropical convective systems and their

contribution to rainfall in Africa (Bouniol et al. 2016; Mathon and Laurent 2001; Mathon et al. 2002; Fiolleau and Roca 2013); the analysis of the trends in their trajectories and characteristics has highlighted their role in the growing occurrence of extreme events in the Tropics (Roca and Fiolleau 2020) and especially in Africa (Taylor et al. 2017).

Rain estimation from IR information is possible; it is however subject to high uncertainties, especially if the information is used at the finer available resolution (Kidd and Levizzani 2011). Gradually since the mid-1970s rainfall measurement techniques based on passive microwave radiometers (PMW) have emerged (Kummerow 2020). Currently, an international constellation of low Earth orbit satellites hosts microwave radiometers that provide rainfall rate estimates every 3 h or more frequently about 90% of the time with spatial resolution of a few tens of kilometers as described by Kidd et al. (2021). The future perspectives and what is foreseen with the ‘New Space’ and constellations of small satellites for frequent revisit of rainfall systems, are also discussed in that review article.

Table 1 provides the main characteristics of the current constellation of fully functional LEO satellites with passive microwave sensors (PMW) used for rainfall estimates. They are part of the Global Precipitation Measurement Mission (GPM) program. This international constellation involves different agencies: the National Oceanic and Atmospheric Administration (NOAA), the United States Department of Defence (U.S.DoD) and National Aeronautics and Space Administration (NASA), the Japan Aerospace Exploration Agency (JAXA) and the European Organization for the Exploitation of Meteorological Satellites (EUMETSAT). The French Centre National d’Etudes Spatiales (CNES) and Indian space Research Organization (ISRO) Megha-Tropiques satellite added a tropical orbit to the constellation, but as it is not fully operational since 2019 is not in Table 1. It can be noted that the constellation is quite heterogeneous (in terms of resolution and frequency channels) which is a challenge for the production of rainfall estimates with regular grid and time steps.

Most applications use freely available multi-satellite rainfall products which are now provided on a regular grid with a nominal resolution of 10 km and hourly time step (Kubota et al. 2020; Huffman et al. 2020). These products use complicated algorithms to combine both the Global Precipitation Measurement mission (GPM) international constellation of passive microwave sensors and geostationary-based IR measurement and may integrate rain gauge information.

Table 1 Characteristics of the current constellation of operational low Earth orbiting satellites hosting passive microwave radiometers for rainfall estimation

Satellite (agency)	Sensors (channels)	Retrieval resolution *
PMW Sounders		
NOAA-19 (NOAA) MetOp-B, -C (EUMETSAT)	MHS (89.0–183.31 GHz)	17.12 km × 21.64 km
NPP, NOAA-20 (NOAA)	ATMS (23.0–183.31 GHz)	16.51 km × 16.22 km
PMW imagers		
GPM (JAXA/NASA)	GMI (10.7–183.31 GHz)	10.9 km × 18.1 km
DMSP F16,F17,F18 (U.S. DoD)	SSMIS (19.35–183.31 GHz)	45 km × 74 km
GCOM-W1 (JAXA)	AMSR2 (6.7–89.0 GHz)	14 km × 22 km

*As given in Kidd et al., 2021; for the sounders the information is for nadir)

Table 2 Characteristics of current operational nadir altimetry satellite mission for measuring water levels

Mission	Jason-CS/Sentinel6	Sentinel3-A	Sentinel3-B
Revisit time	10 days	27 days	27 days
And inter-track distance (at equator)	160 km	104 km	104 km
Period of operation	Late 2020–2026	Early 2016–2023	Mid 2018–2025

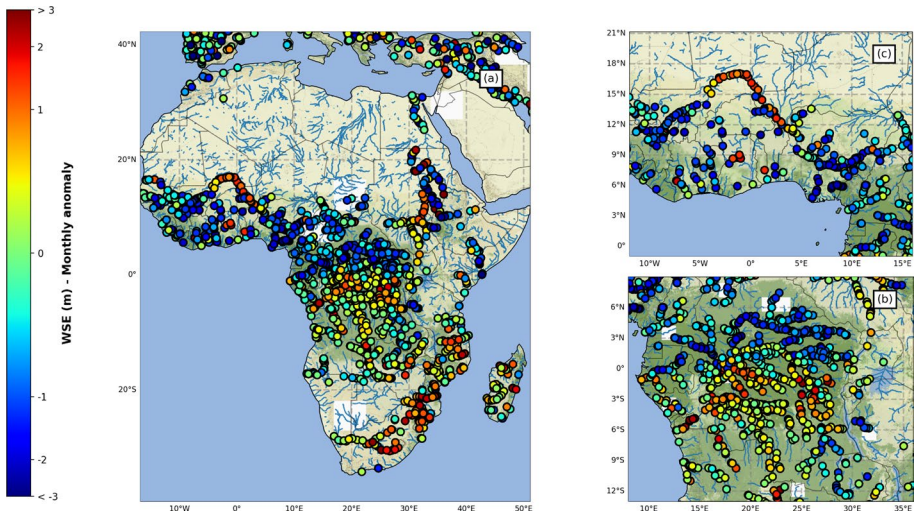


Fig. 1 Illustration of the spatial density of the satellite WSE monitoring network as provided by Hydroweb, and also the temporal resolution of such a database. On the main basins in Africa, there are several tens of observations a week across all the basins, such as the Niger basin (01.b) and the Congo basin (01.c). The hydrological cycle is here clearly identified by the untransformed WSE from altimetry, as attested by the color differences between southern and northern Congo, for example. WSE anomalies (difference from the long-term mean) are identified by the color code, with most negative anomalies in dark blue and most positive anomalies in red

Many studies have shown that these products can provide robust information down to resolution of about 50 km and a few hours (see Gosset et al. 2018; Guilloteau et al. 2016, 2021). Despite tremendous progress in the most recent products, high uncertainties remain in rainfall estimation based on satellite for high resolution (20 km or below and hourly or better) and/or for real-time applications when gauge data are not yet available to improve biases.

Despite these limitations in accuracy and resolution, satellite-based rainfall estimates are extremely valuable for operational applications because they are available at no cost (through dedicated broadcast like EUMETcast, from EUMETSAT) or through simple internet connection), with a global coverage, providing information over both populated and remote areas.

3.2 Monitoring River Water Elevation and Discharge

Rivers water surface elevation (WSE) can be monitored from satellite with radar altimeters onboard. These nadir looking altimeters measure the two-way propagation time of a radar pulse between the satellite and the reflecting water body. Currently thousands of rivers and lakes worldwide are monitored, and the WSE time series are freely available through different web sites (see Table 1 in Papa et al. 2023, in this special issue).

The revisit time of each satellite mission (i.e., the period between two overpasses of the satellite over a given point of the earth surface) and the distance between two Virtual hydrological Stations (VS) on the ground depend on the orbit. For the current operational altimeters, the revisit time ranges from 10 to 27 days as summarized in Table 2. With this constellation, several tens of thousands VS are available in Africa, but the current revisit periods are not adequate for monitoring very fast phenomena such as flash floods.

Figure 1 illustrates the ability of the operational altimeter constellation to provide an overview of the hydrological state of the main African river basins, in one observational cycle. The color dots over the river network (in light blue) indicate whether the river water levels are normal, above (light green-yellow) or below (dark blue) normal for the observation period. This particular example is from January 27th to February 2nd in 2022. A North–South gradient is clearly identified in the Congo basin, with the northern rivers in low flow season and the central and southern tributaries in high flows. The hydrological effect (dumping) of the Niger Inner Delta is also visible, with the upstream tributaries already in low flows, while the Niger main channel downstream is still in high flows.

The dense spatial information provided by nadir altimetry is very valuable for monitoring or studying ungauged or partially ungauged basins (Bogning et al. 2018, Andriambelosom et al. 2020; Kitambo et al. 2021) and also for assessing the quality of hydrological and hydrodynamic models (Paris et al. 2020), or calibrate their parameters (O’Loughlin et al. 2019). This type of observation is extremely useful for the management of trans-boundary basins when data sharing is an issue.

The WSE is measured by the satellite with respect to a reference ellipsoid or the geoid. They need to be converted to local height references, river depths or discharges, in order to be used in applications. To do so, the WSEs are used jointly with other remotely sensed variables or/and hydrological models through rating curves or empirical relationships, as detailed in Tarpanelli et al. (2023, in this issue). Since the operational availability of nadir altimetry missions thanks to the EC Copernicus program and the near-real-time (NRT) provision of WSE, new applications of these data for basin monitoring, discharge prediction and early warning systems based on flow peak propagation have been developed. Section 4 provides an illustration of this potential, with the record flood case of the Ubangui river in 2019.

3.3 Mapping Flood Extent

The most commonly used satellite data sources for the delineation of flood extents are optical and Synthetic Aperture Radar (SAR) data. Optical sensors are passive and measure the solar radiation reflected by the Earth surface in the visible and infrared frequency bands. This type of images is easily interpreted by the human eye. However, they require solar illumination and cloud-free atmosphere to provide Earth surface observations. This limits the use of optical images for flood monitoring as flood events may occur at night and are often associated with cloud cover. Synthetic Aperture Radar (SAR) sensors are active

Table 3 Examples of current and past satellite SAR missions used for flood monitoring

Satellite mission	Wavelength (cm)	Life status	Resolution (m)	Repeat cycle (days)	Swath width (km)
<i>L Band</i>					
J-ERS	23.5	1992–1998	18	44	175
ALOS PALSAR	23.6	2006–2011	10–100 m	46	70–350
ALOS PALSAR 2	22.9	2014	3–100	14	25–490
SAOCOM	23.5	2018	10–100	8–16	14–235
<i>C Band</i>					
ERS-1/2	5.6	1991–2001	10–30	35	5–100
ENVISAT	5.6	2003–2010	25–1000	35	5–400
RADARSAT-1	5.5	1995–2013	10–100	24	45–500
RADARSAT-2	5.5	2007	3–100	24	50–170
Sentinel-1	5.6	2014	5–20	6–12	20–400
Gaofen-3	5.6	2016	1–500	26	10–650
RADARSAT Constellation	5.5	2018	3–100	12	30–350
<i>X Band</i>					
COSMO-SkyMed	3.1	2007	1–30	2, 4, 8, 16	10–200
TerraSAR-X/Tandem-X	3.1	2007	1–20	11	10–100
KOMPSAT-5	3.2	2013	1–20	28	5–100
PAZ	3.1	2018	1–20	11	5–100

side-looking sensors. They send a microwave signal toward the Earth’s surface and measure the signal that is backscattered toward the satellite. SARs can image the Earth surface day and night and through cloud cover, making them very relevant for flood extent mapping. The main limitation of optical and SAR satellites for imaging inundation is their long revisit time, typically a few days, meaning that the onset of some dangerous phenomena or

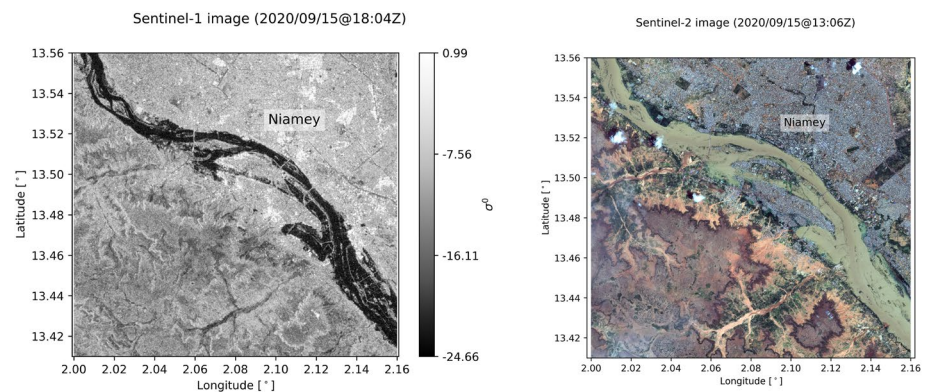


Fig. 2 Example of two Sentinel-1 and 2 flood images acquired over Niamey on August 15, 2020: Sentinel-1 (SAR) image on the left panel and Sentinel-2 (Optical) image on the right panel

Table 4 Examples of current satellite optical missions used for flood monitoring

Satellite mission	Life status	Resolution (m)	Repeat cycle (days)	Swath width (km)
Modis (Terra-Aqua)	1999	250–1000	16	> 2000
Landsats-7–8	2013	15–30	16	180
Sentinel-2	2015	10–60	10	290
Worldview-4	2016–2019	0,3–14	–	13
Spot 6–7	2014	1,5	26	10
Pléiade	2011	0,5–2	26	20

short lasting flood events may be missed. Over the last decades, the number of SAR satellite missions has increased, enabling a substantial reduction of revisit time. For example, the Cosmo-SkyMed SAR sensor can be pointed toward a predefined area of interest on demand and revisit it as frequently as daily. The programming of satellites of course comes at a cost to the user. The Sentinel-1 mission (2015) provides worldwide free of charge SAR images at 20 m spatial resolution with frequent revisit times (see Table 3). Conversely to commercial satellites such as Cosmo-SkyMed or TerraSAR-X that can be programmed (i.e., pointed toward a predefined area), Sentinel has a fixed acquisition plan, meaning that acquisitions are more systematic and therefore enable the exploitation of change detection or images time series-based approaches. Figure 2 shows as an example a couple of SAR and optical Sentinel-1 and 2 satellite images acquired the same day over the same area.

Table 3 and Table 4 list the SAR and optical satellite missions that are most often used for flood mapping. The repeat cycle indicated for each satellite is between two overpasses of a given orbit. As images acquired from different orbits can substantially overlap depending on the latitude of the area of interest, the effective revisit time for a given point may be substantially shorter. For example, over Europe, the revisit time of Sentinel-1 images can be as short as 1 day.

The detection of open water bodies in rural and peri-urban areas is rather straightforward on SAR and optical images due to their specific responses. In SAR images, open water appears with very low backscatter due to specular reflection on the smooth water surface. Many approaches have been proposed to detect water in SAR images. Some of them are fully automated and unsupervised (e.g., Martinis et al. 2015), enabling fast and reliable water detection. They often rely on histogram thresholding, region growing and/or change detection based on a pair of images, one taken before and one during the flood (Landuyt et al. 2019). In optical infrared images, water has a distinctive spectral signature for example very dark in near infrared (NIR), red and green bands. Many band combination indices have been proposed such as the Normalized Difference Water Index (NDWI, McFeeters 1996) to detect water. These indices enhance the contrast between water and the rest of the image, for better detection. The resulting flood maps are often provided as binary maps, but may also include probability and/or uncertainty information (e.g., Giustarini et al. 2016; Sherpa et al., 2020). Some studies have proposed methods (e.g., Schumann et al. 2007, Hostache et al. 2009, 2010; Mason et al. 2014) for estimating water levels or depths combining flood extent boundaries derived from SAR images and topography data, with good levels of accuracy (elevation error $\sim \pm 50$ cm when high resolution, high accuracy datasets are used).

As of today, optical and SAR images are operationally used, in near-real time, for monitoring extreme flood events around the world for example in the framework of the

International Charter Space and Major Disasters (<https://disasterscharter.org>) and the Copernicus Emergency Management Service (<https://emergency.copernicus.eu/>). These operational services (launched upon request of authorized member states or agencies when a large flood event is identified) provide, within a few hours after the satellite acquisition, flood extent maps derived from all available Earth observation satellite missions (see Tables 3 and 4) that are very useful for organizing rescue operations, estimating damages or reanalyzing the event (Matgen et al. 2020). The Copernicus Emergency Management Service is currently developing a free operational service that will offer in near-real-time (within the 8 h following any Sentinel-1 image acquisition) flood and water extent maps, along with additional related quality and uncertainty products, automatically derived from any Sentinel-1 image acquired around the world.

Detecting water in urban areas where emerging buildings can mask water from space is more challenging, especially for side-looking SAR sensors. New methods based on SAR interferometry are very useful in this respect. For example, the approach proposed by Chini et al. (2019) and further developed by Pelich et al. (2022) uses pairs of Interferometric Sentinel-1 images acquired before and during the event to detect buildings affected by flood-water using the phase coherence drop due to the arrival of water in front of those buildings.

Unfortunately, despite the recent developments in flood mapping, especially using SAR data, some water bodies are still undetectable, for example under dense vegetation or in the building- and topography-induced shadow areas. To identify these areas where water cannot be detected, recent methods (e.g., Zhao et al. 2021) analyzed long time series of SAR data and provide an exclusion map dedicated to flood mapping.

3.4 Integration with Flood Models

Remotely sensed flood information can be integrated with flood models, such as one-dimensional and two-dimensional hydrodynamic/hydraulic models, through model

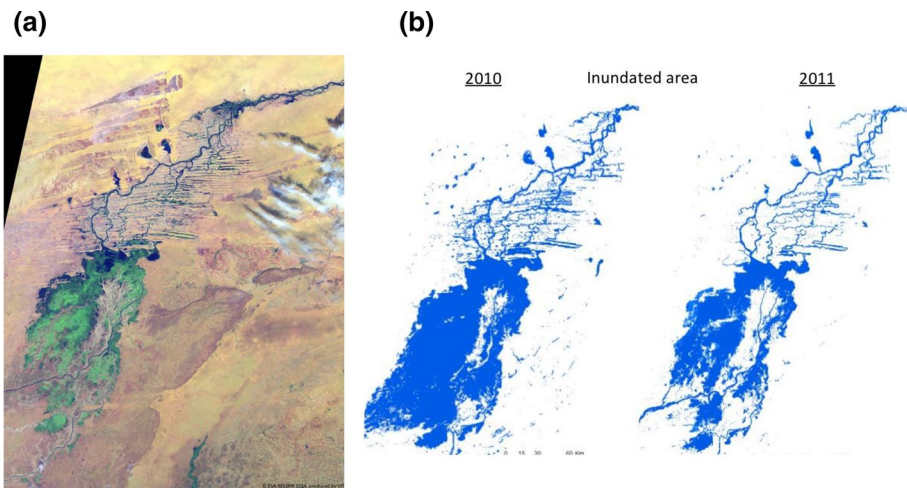


Fig. 3 Illustration of inundation pattern of the Niger Delta in Mali. **a** a Landsat image of normal wet conditions and **b** simulations of a wet (2010) and a normal (2011) year by the two-dimensional subgrid model introduced by Neal et al. (2012)

calibration, validation or data assimilation. Flood models simulate water flow volumes and depths within channel networks and in the adjacent floodplain lands. Such approaches are needed for predicting inundation as well as for flood event re-analysis and flood hazard estimation.

As described in the previous sections, satellites can provide information about both flood area and water levels, albeit with various levels of accuracy. A variety of methods exist to integrate such information with flood models. As already noted, the most common use of flood area or extent information is for model calibration or validation (see, e.g., Aronica et al. 2002, a landmark study example).

Model calibration can be defined as the process of adjusting model parameters in order to optimize the fit between model simulations and observations. Validation, or verification, involves comparing model output with observations and using this to deduce model performance (Fig. 3).

The study by Neal et al. (2012) is a notable example, integrating EO data and a large-scale flood model. Their model employs a sub-grid channel structure to approximate channel bathymetry based on a simple but well-established relationship between river discharge and channel width and depth. This particular setup was first used to simulate flood inundation in the large inland delta of the Niger River (Neal et al. 2012). The model was successfully calibrated with in-channel water levels observed by the ICESat-1 satellite, which were derived following the method introduced by (Hall et al. 2012). After calibration, the model performance was validated using Landsat-5 imagery of the wet and dry season in the delta region (Fig. 3). The same type of flood model and similar remote sensing data, i.e., ICESat-1 and Landsat, among other satellite imagery of flooding, were also used by Schumann et al. (2013) to calibrate and validate, respectively, a coupled hydrologic-hydraulic flood inundation forecasting model of the Lower Zambezi basin in South Eastern Africa. In this case study, the remotely sensed data proved especially useful during calibration to constrain the large uncertainty in the model outputs due to the large spread in inflow forecast uncertainty.

It is worth noting that the above-reported case study was successfully undertaken in a region largely deprived of good-quality topography or long-term high-quality discharge measurements. This situation is true for many regions around the world and often prevents or limits the development of accurate flood hazard and risk models let alone operational flood forecasting systems.

Recent studies have also proposed methods for directly assimilating flood extent maps derived from satellite imagery using variational methods (e.g., Lai et al. 2014), ensemble Kalman filters (e.g., Cooper et al. 2019) or particle filters (e.g., Hostache et al. 2018, Dasgupta et al. 2021a, b, Di Mauro et al. 2021). The study by Di Mauro et al. (2022) for instance showed in a synthetic experiment that the sequential assimilation of flood extent maps derived from Sentinel-1 SAR images can reduce on average by 80% the error of forecast water level. Although the proposed methods were not applied in Africa yet, they hold promises as the aforementioned studies all show that the assimilation of flood extent maps helps reduce flood prediction and forecasting model uncertainty either via parameter, state variable or forecast updating, especially in data scarce areas.

Altimetry-derived discharges can also be assimilated into hydrological, hydrodynamic and hydraulic models in order to improve the nowcast and forecast skills of these models. Even though WSE could directly be assimilated, it is preferred to assimilate discharge to overcome biases or geometry issues. Recent studies (Pujol et al. 2022; Malou et al. 2021, among others) in South American basins where many in situ gauges could be used for

validation, proved that satellite altimetry assimilation can improve discharge predictions and, consequently, floods and droughts predictions.

4 Case Studies/Examples: Recent/Major Floods Events in Africa Revisited Through Spatial Observations

4.1 Beira 2019 Case Study

In March 2019, Cyclone Idai hit Mozambique and was responsible for major flooding in many provinces including Inhambane, Manica, Sofala, Tete and Zambezia. The cyclone was particularly devastating and impacted the region in three phases (OCHA 2019). In the first days of March, more than 140,000 people were displaced due to large inundation in Zambezia and Tete resulting from heavy rainfall due to the antecedent low-pressure system. Later on, in mid-March, the cyclone caused landslides around the port of Beira, with many more casualties and damages. In the final stages, heavy rainfall caused the rivers and streams to overflow. It was reported that 1.85 million people needed humanitarian assistance and protection. The authorities estimated that nearly 112,000 houses were impacted, leaving more than 131,000 people displaced.

Satellite Earth observations are useful for monitoring and managing such large-scale events, as they provide synoptic observations over very large areas, and help identify the most affected areas.

Figure 4 shows two different maps derived from Sentinel-1 imagery during the 2019 flood event in Eastern Mozambique. The top panel of Fig. 4 is the maximum observed inundation extent derived from Sentinel-1 data acquired between as of March 20, 2019 at 03:08 UTC. It was obtained by summing the flood extent derived from a time series of Sentinel-1 images acquired between March 2 and March 20 using the method described in Chini et al. (2019). This map identifies the flooded area across the previously mentioned event phases over Mozambique and shows the magnitude of the event. The bottom panel of Fig. 4 is the flood extent and the impacted building map as of 20/03/2019 at 03:08 UTC. The flooded areas were derived using the method described in Chini et al. (2019). The affected buildings were detected using the method proposed in Chini et al. (2019) that relies on the detection of interferometric coherence drop in front of the buildings due to the appearance of water. In other words, the affected building map identifies open water areas located on the side of the building illuminated by the SAR signal.

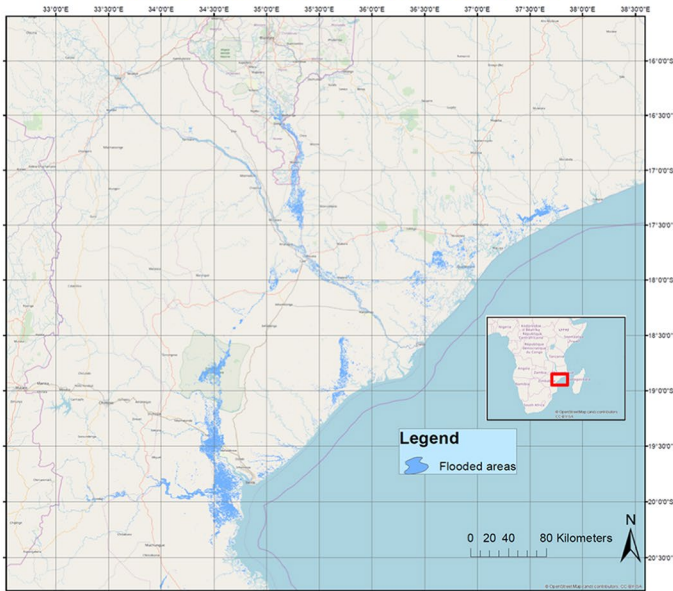
As can be seen in Fig. 4, a substantial part of Beira is identified as flooded using Sentinel-1 interferometric data, extending detection capacity to urban, peri-urban and rural areas.

Figure 5 also shows a very high-resolution optical image acquired by the Worldview satellite on March 29, 2019. This partly free of cloud flood image enables to identify significant flooding at the street level.

4.2 The Case of the Recurring 'Red Floods' Phenomena in Niamey and the Record 2020 Flood Captured by a Hydrological Model and Real-Time Rain Product

The 2020 hydrological season was exceptionally intense in Africa. In September, the highest level of the Niger river since the beginning of observations was recorded in Niamey. What happened in 2020 in Niamey is the ultimate example of a phenomena which has been

**Maximum observed inundation extent derived from Sentinel-1 data
acquired between 02/03/2019 and 20/03/2019**



**Inundation extent and impacted buildings derived from Sentinel-1
data acquired on 20/03/2019 at 03:08 UTC**

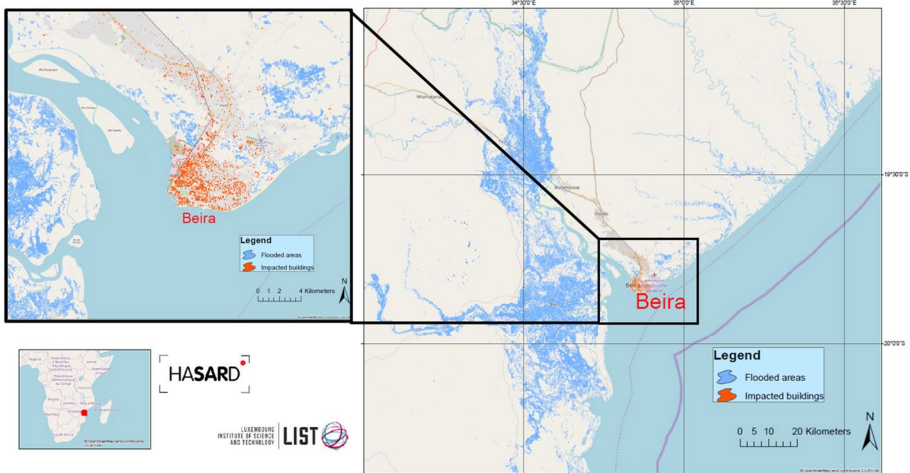


Fig. 4 Flood extent and affected building maps derived from Sentinel-1 imagery during the 2019 flood event in East Mozambique. Top panel: maximum observed inundation extent derived from Sentinel-1 data acquired between March 2, 2019 and March 20, 2019. Bottom panel: inundation extent and impacted buildings derived from Sentinel-1 data acquired on March 20, 2019 at 03:08 UTC

growing in the last two decades in the middle Niger basin (Massazza et al. 2021; Casse et al. 2016).



Fig. 5 Example of a partially cloud-free very high-resolution image of the devastating flooding in the port city of Beira during Tropical Cyclone Idai. This post-event WorldView flood image of Maxar was acquired on March 29, 2019 (source: Open Data Program © Maxar). Note the difficulty in separating the flooded brown-colored areas from the unflooded brownish soils



Fig. 6 River Niger in flood around and in Niamey in September 2020. (Photograph courtesy Niger Basin authority, NBA)

The Niger river at its middle basin experience two annual peaks: (i) The Sahelian flood—also called red flood—occurs during the rainy season, between August and September mainly from the inflows of the right bank tributaries upstream of Niamey (Goro-uol, Dargol and Sirba). “Red” refers to the color of the water loaded in iron oxide sediment, brought carried by these three Sahelian tributaries. (ii) The Guinean flood—or black flood—occurs later in the season, between November and February. It is generated by rains occurring in the upper basin watersheds located in Guinea and Mali, upstream of the Niger Inner Delta. The long time lag between the rainfall season in Guinea (May to September) and the arrival of the peak in Niamey (November–February) is due to the propagation time along the river course and the dampening effect of the Niger Inner Delta (Fig. 6).

Historically the “black” flood had the highest peak, but progressively over the last 3 decades, the “red” peak began to surpass the black one and has been the cause of a succession

of record floods since 2012 (Casse et al. 2016). This evolution in the hydrological behavior of the middle Niger basin is the consequence of long terms changes in the land surface superimposed with the occurrence of intense precipitation over the three Sahelian tributaries basins. The timing and the intensity of the red floods are related to the dynamics of the rainfall systems crossing this relatively small drainage area (about 50,000 km²). Casse et al. (2015) showed that the red floods could be reproduced using a distributed hydrological model and satellite rainfall product as forcing. Based on these initial results, a modeling platform was developed in collaboration with the Niger river Basin Authority (NBA) with the objective to monitor the state of the river and help anticipating flood risk. The platform is based on a distributed, coupled hydrodynamical-hydrological model called MGB (Fleischmann et al. 2018). The rain forcing is updated daily using the real-time rainfall product GSMAP (Kubota et al. 2020) since 2017. With a spatial resolution of 0.1° the product is compatible with the resolution (10 km) of the model's elementary hydrological units (Fleischmann et al. 2018).

Figure 7 shows the spatial patterns of daily rain accumulations for the strongest rain events (highest rain volumes) that contributed to the red flood peaks in August and September 2020. Runoff due to these intense systems occurred in the three tributary basins, located mostly in Burkina Faso, North–West of Niamey.

Figure 8 (from the pilot real-time monitoring web site: <https://mgb-hyfaa.pigeo.fr/>) displays the domain covered by the MGB model. The three tributaries responsible for the red flood rise are located just upstream of Niamey, with their drainage area located mostly in Burkina Faso. The time series of discharge simulated and observed (in situ) in Niamey are displayed, both exhibiting record levels in 2020. The water levels observed with altimetry (Fig. 8b) upstream, close to Niamey, are also showing a strong positive anomaly (of about 1 m) in 2020, consistent with the local observations. An altimetry data assimilation scheme is currently being tested with the model in order to improve the predictions.

As an illustration of the capabilities of Sentinel images for flood extent mapping, Fig. 9 shows two flood extent maps derived from two Sentinel images (Sentinel-1 and Sentinel-2) acquired over Niamey in September 15, 2019. The corresponding satellite images that were used as input are shown in Fig. 2. The flood extent was derived from the Sentinel-1 image using the method proposed by Chini et al. (2019) and from the Sentinel-2 image using the one proposed by Pulvirenti et al. (2021). As can be seen in Fig. 9, the flood extent derived from the SAR imagery is smaller than that derived from the Sentinel-2 imagery. This is mainly due to the emerging vegetation at the shoreline that substantially increase the radar backscatter as a result of multiple bounce reflection and makes it more difficult to identify in SAR images with traditional algorithms.

4.3 Ubangui 2019: Peak Flow Propagation over a Major African River Anticipated by Altimetry

In late 2019 (October and November), the Ubangui River basin, one of the main tributaries of the Congo River, was hit by a high-magnitude flood event after years of relatively low peaks (Nguimalet and Orange, 2019). The flood caused thousands being displaced (Floodlist 2019) and several buildings to collapse. The event was caused by heavy rainfall in the upper part of the basin and caused overbank flooding in several parts of the lower basin. This flood was totally unpredicted because no in situ gage is available upstream nor any early warning system.

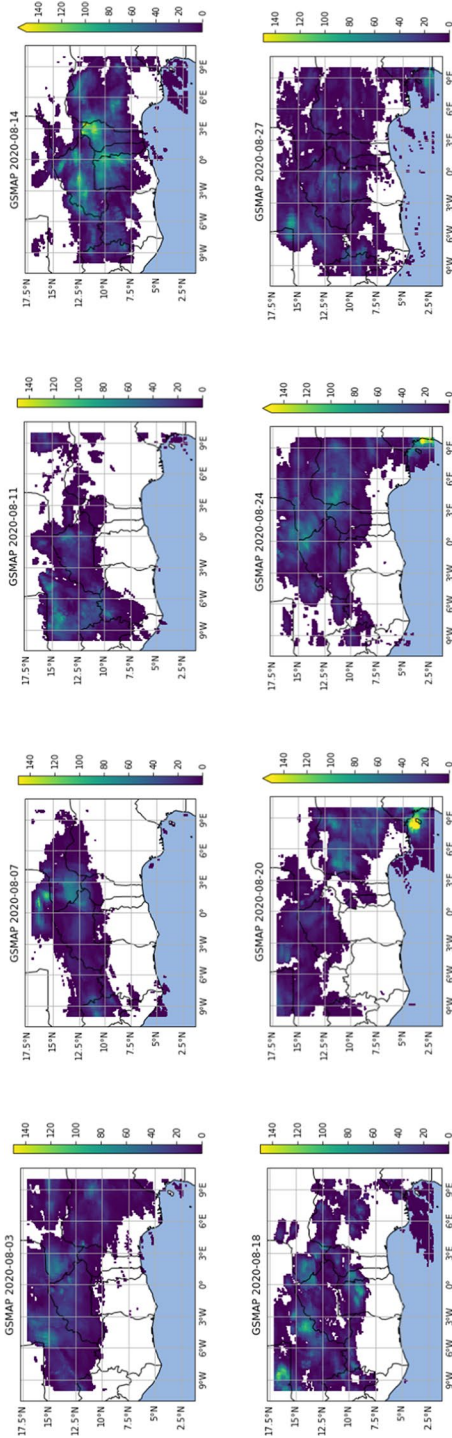


Fig. 7 High-resolution daily rain maps from the GSMAP satellite product for the main rain events in August 2020, responsible for the record red floods

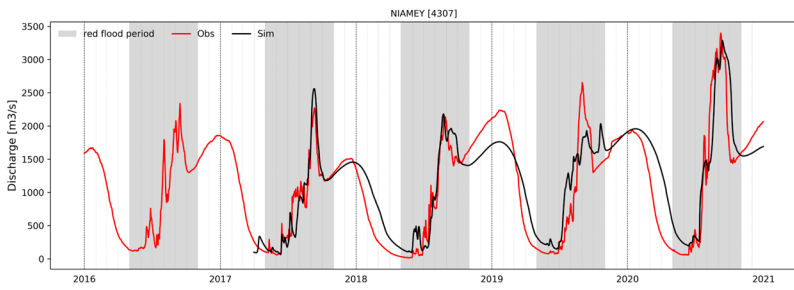
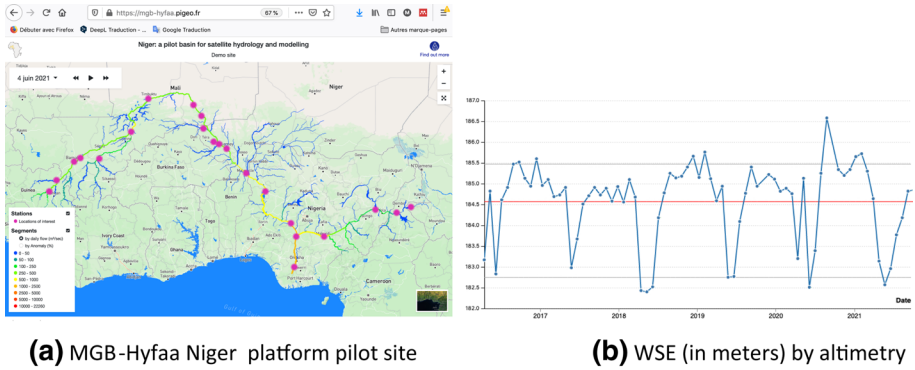


Fig. 8 The modeling platform MGB-HYFAA set up for the Niger River and operating in real time (daily update). **a** Domain covered, **b** series of WSE (meters) by the altimetric virtual station located 30 km upstream Niamey on the Niger river, **c** simulated and observed discharge in Niamey over the period 2017–2020, exhibiting the record level in 2020. The gray shading shows the period where the ‘red’ flood occurs

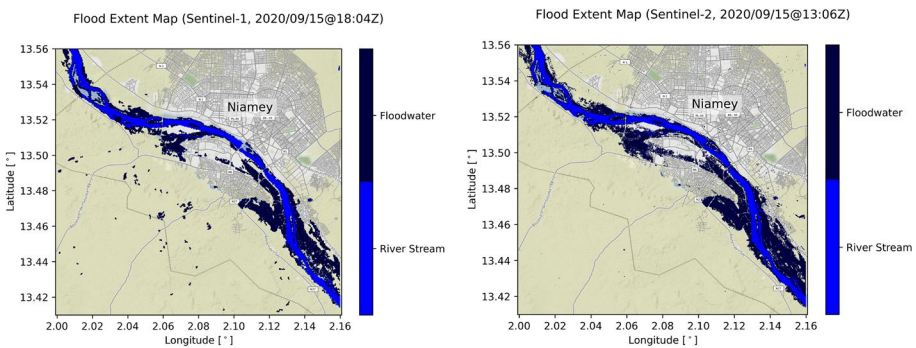


Fig. 9 Flood extent maps derived from two sentinel images (Sentinel-1 on the left, and Sentinel-2 on the right) acquired over Niamey on September 15, 2019

The operational altimetry constellation was composed in 2019 of Sentinel-3A&B and Jason-3, which represent almost two hundred VSs on the Ubangui and its main tributaries (Kotto, Mbomou, Uele and Bomokandi), already available on Hydroweb [<https://hydroweb.theia-land.fr/>], and many more to be processed. If a single VS, located right upstream

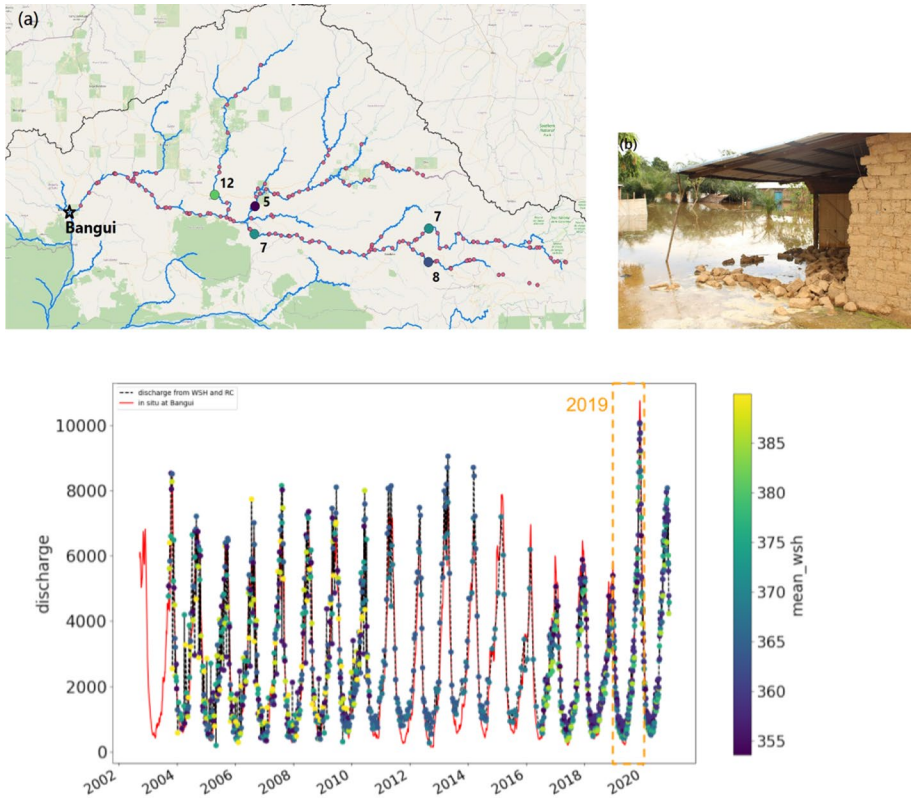


Fig. 10 **a** Upper panel: map of the Ubangui River basin main streams (blue line) together with the operational virtual stations from Hydroweb (small pink dots); the correlations lag time between the MGB simulation at Bangui and downstream of each main tributary is provided by the larger blue-green colored dots and indicated next to the dots, from dark blue (5 days) to light green (12 days). **b** Lower left: the 2019 flood near Bangui (credit: CRCA); **c** time series reconstructed at Bangui from 2004 to 2020 using a combination of WSE time series from different VS upstream that are converted into discharge using lagged rating curves (Paris et al. 2020). The exceptional year 2019 is highlighted by the orange dash framing. The red line is the in situ discharge time series from the HybAm observatory (<https://hybam.obs-mip.fr>). Each dot is colored as a function of the mean WSE of the original VS it is derived from (also related to its distance from the outlet: blue, high mean WSE, near the Bangi outlet; yellow, far upstream in smaller tributaries)

Bangui, may be insufficient to catch the flood peak due to the time sampling and even less to help mitigate its effects, several VSs located upstream can be combined to provide information on the overall processes occurring in the upstream basin.

Figure 10 illustrates how the current altimetry constellation could have been used to monitor and anticipate the 2019 flood at Bangui. Figure 10a displays VSs from each tributary of the Ubangui River that can be used as predictor. The colors of the dots indicate the mean time lag between the flood pulse at Bangui and the pulse upstream (and earlier) at the virtual station. They were calculated from lag correlation analysis. The high correlations (>0.9 for Kotto, Mbomou and the lower Uele, and >0.85 for the upper Uele and Bomo-kandi) between the fluxes upstream and the discharge at Bangui suggest a good prediction potential and show that the extreme event was detected upstream before reaching Bangui. Combining the VSs time series from upstream (each with a lag and an appropriate rating

curve as explained in Paris et al., 2020), the time series at Bangui (Fig. 10c) was reconstructed. The exceptional levels reached in 2019 are visible. Thanks to this method a continuous time series is obtained in Bangui despite the fact that the VS closest to this station did not catch the flow peak due to sparse temporal sampling.

This example provides a simple framework for anticipating extreme flood events in ungauged catchments using only the current operational altimetry constellation. In ungauged basins, such as the Ubangui River basin, this constellation offers a great opportunity for monitoring and even mitigating events. Future missions should improve the system by providing more accurate and/or more frequent observation of WSE and discharge. The WSE observations also offer great potential to be combined with other types of observation, such as flooded areas, to improve the timeliness of alerts.

4.4 Abidjan—Satellite Data for Classifying Risk-Prone Areas and Rainfall Systems

During the rainy season, each year, several districts of Abidjan, the capital of Côte d’Ivoire, are flooded. The floods cause material damages and casualties every year (21 in the 2009 season and 18 in the 2018 season). Studies have shown that 26% of Abidjan City can be classified as ‘at risk’ and the population growth (about 5% per year) worsen the situation. The floods are caused mainly by intense rainfall over the very city; their effect is worsened by the clogging of rainwater pipes and drainage by waste. The associated damages and casualties could be avoided through better planning. Satellite information can help nowcast the

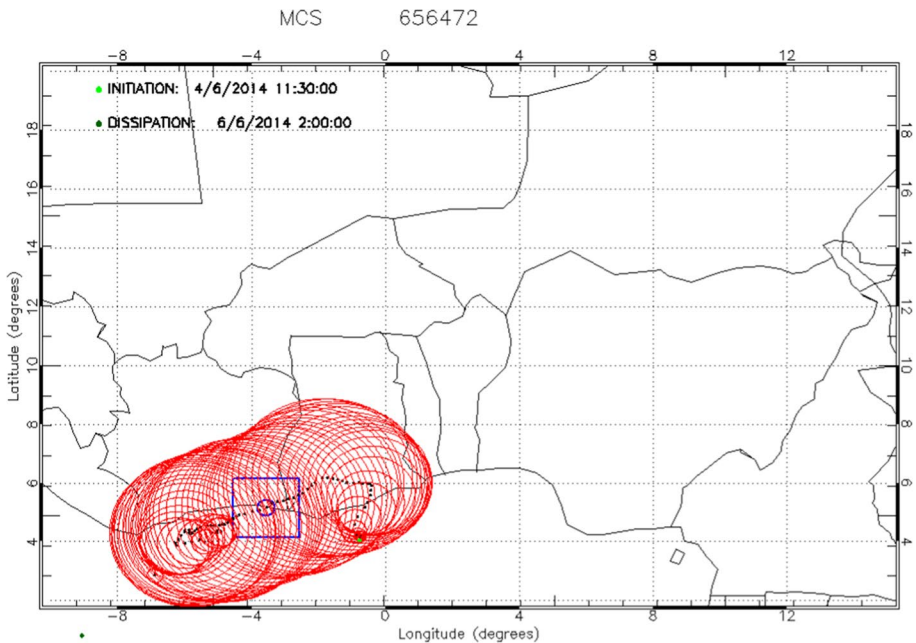


Fig. 11 Analysis of the trajectory and dimensions of the mesoscale convective system (MCS) that caused pluvial flooding in Abidjan during June, 4–6 2014. The MCSs were tracked using the TOOCAN (see text) product and geostationary (IR) data

severe storms that may cause floods and can provide some information to better locate the populations that are most exposed to the risks.

Studies are being carried out in order to help short-term prediction (a few hours) of these floods events based on the tracking and characterization of the mesoscale convective cloud systems (MCSs; Fiolleau and Roca 2013; Mathon and Laurent 2001). Such a tool could provide very valuable information to the mandated services and authorities, for informed decision making.

Based on a five-year analysis of MCS characteristics (area; minimum brightness temperature; total time life of the system) and flood damage information (from civil security services), it was found that the most damaging systems are short lived and localized (Fig. 11). These results contrast with what has been observed in the Sahel, where extreme rainfall is associated with long-lasting systems with large areal extents, and very high/cold cloud tops (Roca and Fiolleau 2020; Taylor et al. 2017). They confirm the potential interest of satellite information for a regionalized analysis of extreme events, to better inform authorities.

Once the severe rainy events have been detected and their trajectory is surveyed, the population from areas most at risk can be alerted. Satellite information (high-resolution optical images) can be used (together with post-crisis data from local surveys) to map the area where the populations are at most risk, based on socio-economic criteria and information on houses and other relevant infrastructure; Fig. 12 shows vulnerability maps derived from this technique (ongoing work).

5 Conclusions and Perspective

The occurrence of pluvial and fluvial floods in Africa has been increasing and this trend is expected to continue, because climate change is associated with the intensification of the water cycle, and because the changes in land use and the urbanization increase the hydrological impacts of extreme weather events. These floods have consequences on the ecosystems, on the agriculture and livestock, on homes and infrastructures, on the economy and above all, they can also many deaths. While some people die from drowning or are swept away by floodwaters, others see their homes become uninhabitable or even destroyed. Abandoning their homes, the shortage of drinking water and food is added to the consequences directly affecting people. The great devastation that a flood leaves behind is also conducive to the spread of diseases with waste and water-related diseases. It is therefore

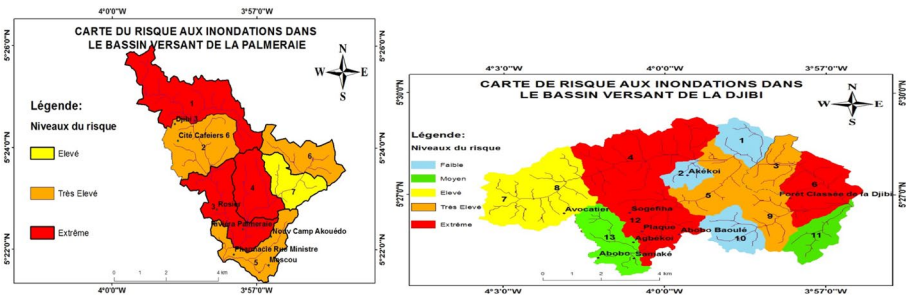


Fig. 12 Flood risk maps derived from optical images and supervised classifications for two of the most vulnerable districts in Abidjan

urgent to define effective policies with a comprehensive approach to flood management at the local and national levels—and also at the regional level as storm and rivers propagate through borders, and population affected by natural disasters often migrate. These policies should bring together the numerous existing measures with the objectives of reinforcing the safety of the population (monitoring, particular vigilance in the case of seasonal and/or exposed activities), reducing the cost of damage (anticipating and managing the crisis) and shortening the time required for the return to normalcy of the affected areas. To act and react, the mandated authorities and agencies involved in flood risk reduction must have information on past, current and future flood risk. Given the overall deficit of hydrometeorological data across the African continent, satellite observations can play a crucial role in documenting floods, their causes and their foreseen evolutions.

This review presented a multitude of satellite data and methods which are currently used to analyze and predict floods: rainfall monitoring and estimation from satellite is used to monitor extreme weather events and also as forcing data of hydrological (rain-discharge) models in order to predict discharge, and associated flood risk; satellite altimetry is useful to detect anomalous high water levels or can be assimilated in prediction models; optical and SAR images can measure the extent of flooding, a useful piece of information for direct monitoring or for assimilation in hydrodynamic models; high-resolution optical images are interesting for mapping vulnerable and damaged areas.

The concrete application of these techniques to monitor extreme events and flood risk in Africa was illustrated by revisiting several recent flood use cases that caused much damage. The exceptional floods that followed the passage of Cyclone Idai in Mozambique, in 2019 were well observed by SAR imagery; they were used to map the flooded areas and guide rescues to the most affected zones. Later in 2019, the Ubangui River, one of the main tributaries of the Congo River, was hit by a strong flood wave due to heavy rainfall in the upper part of the basin that caused overbank flooding; the propagation of the exceptionally high peak along the river was well measured by satellite altimetry and an early warning system based on these observations could be implemented on this basis. Niamey, the capital of Niger, has been subjected to intense flooding regularly over the last decades; these so-called red floods are caused by intense runoff when mesoscale convective systems propagate over three Sahelian tributaries just upstream of Niamey; the absolute record 2020 flood was well simulated by a hydrological model that used real-time satellite rain products as forcing. Abidjan is regularly hit by pluvial flooding during the rainy season, every year. The storms that cause most damage can be tracked in time and characterized by geostationary satellite data; the most vulnerable areas can be mapped with optical imagery.

Despite successful usage of satellite information for flood analysis in Africa, there are some limitations to the current data and methods. The very small spatial and temporal scales associated with urban flash floods are still a challenge for the current observing systems. The constellation of satellites currently dedicated to rainfall is denser than ever, with about a dozen passive microwave sensors (the GPM constellation), two radars (GPM DPR and Cloudsat) and high-resolution, multispectral geostationary satellites (Kidd et al. 2021). However, the effective resolution of the products based on the constellation is around 50 km, 3 h (Guilloteau et al. 2021) even if their nominal resolution is hourly/10 km. Going down to smaller scales would necessitate new algorithmic approaches or constellation of sensors allowing more frequent revisit while keeping high resolutions. Some perspectives could be offered in that direction within the emerging commercial ‘New Space’ and the prospect of less costly and more compact small satellites.

One current limitation of the altimetry data for operational hydrology and flood risk monitoring, is the relatively low revisit time of the current constellations. Blumstein et al.

(2019) are proposing a potential constellation of ten small altimetry satellites dedicated to continental surface waters (SMASH mission) which could offer a daily revisit capability (interorbit distance 250 km). The analysis of the benefit of such a mission for the flooding hot spots of the main African rivers (especially Niger) is underway using Observing Systems Simulation experiments (OSSEs) and a data assimilation framework.

The current data-rich environment on flood inundation observations will be further strengthened with new, upcoming and potential satellite missions dedicated to flood hydrology. ESAs Sentinel-1 synthetic aperture radar (SAR) mission is targeted at operational applications and the National Aeronautics and Space Administration/Centre National d'Etudes Spatiales (NASA/CNES) SWOT mission (which was launched on 17 of late December 2022) would measure water levels at 25 cm accuracy for an area of 250 m×250 m (Biancamaria et al. 2016) and would potentially provide a global water database including river and lake area and width, inundation area and water heights, water surface slopes and even characterization of discharge (Biancamaria et al. 2016; Wong-chuig-Correa et al. 2020; Schumann and Moller 2015). Public missions are constantly being complemented by satellite missions from private sector industry that are launching a high number of small satellites or cubesats, such as Maxar, Planet Labs, Capella, Spire Global and many others (Fig. 5). The “New Space” industry is rapidly growing and with it many new opportunities are appearing. The proliferation of satellite data of course requires a parallel growth of big data analytics using online cloud computing platforms and machine-to-machine enabling technology.

Acknowledgements The work of RH was funded by the Luxembourg National Research Fund (FNR) through the CASCADE project (Grant No. C17/SR/11682050). The project in Ivory Coast is funded by the Education and Research Ministry of Côte d'Ivoire, as part of the Debt Reduction-Development Contracts (C2Ds) managed by IRD (French National Research Institute for Sustainable Development)—Grant : 5768A1-PEV". The project in Niger is partly funded by Agence Française de Développement (AFD). MG, AP and LG work is partly funded through the Centre Nationale d'Etudes Spatiales (CNES) through the TOSCA program. The authors would like to thank the Autorité du Bassin du Niger (ABN) for providing in situ data and their expert knowledge on the Niger river hydrology.

Data Availability Statement Data supporting the figures are available via the indicated references (articles or websites) or by contacting the corresponding authors.

Open Access This article is licensed under a Creative Commons Attribution 4.0 International License, which permits use, sharing, adaptation, distribution and reproduction in any medium or format, as long as you give appropriate credit to the original author(s) and the source, provide a link to the Creative Commons licence, and indicate if changes were made. The images or other third party material in this article are included in the article's Creative Commons licence, unless indicated otherwise in a credit line to the material. If material is not included in the article's Creative Commons licence and your intended use is not permitted by statutory regulation or exceeds the permitted use, you will need to obtain permission directly from the copyright holder. To view a copy of this licence, visit <http://creativecommons.org/licenses/by/4.0/>.

References

- Andriambelosen JA, Paris A, Calmant S, Rakotondraompiana S (2020) Re-initiating depth-discharge monitoring in small-sized ungauged watersheds by combining remote sensing and hydrological modelling: a case study in Madagascar. *Hydrol Sci J* 65:2709–2728. <https://doi.org/10.1080/02626667.2020.1833013>
- Aronica G, Bates PD, Horritt MS (2002) Assessing the uncertainty in distributed model predictions using observed binary pattern information within GLUE. *Hydrol Process* 16:2001–2016. <https://doi.org/10.1002/hyp.398>

- Berne A, Krajewski WF (2013) Radar for hydrology: unfulfilled promise or unrecognized potential? *Adv Water Resour*. <https://doi.org/10.1016/j.advwatres.2012.05.005>
- Biancamaria S, Lettenmaier DP, Pavelsky TM (2016) The SWOT mission and its capabilities for land hydrology. *Surv Geophys* 37:307–337. <https://doi.org/10.1007/s10712-015-9346-y>
- Blumstein D, Biancamaria S, Guérin A, Maisongrande P (2019) A potential constellation of small altimetry satellites dedicated to continental surface waters (SMASH mission). 2019: H43N-2257
- Bogning S, et al. (2018) Monitoring water levels and discharges using radar altimetry in an ungauged river basin: the case of the Ogooué. *Remote Sens*. <https://doi.org/10.3390/rs10020350>
- Bouniol D, Roca R, Fiolleau T, Poan DE (2016) Macrophysical, microphysical, and radiative properties of tropical mesoscale convective systems over their life cycle. *J Clim* 29:3353–3371. <https://doi.org/10.1175/JCLI-D-15-0551.1>
- Casse C, Gosset M, Peugeot C, Pedinotti V, Boone A, Tanimoun BA, Decharme B (2015) Potential of satellite rainfall products to predict Niger River flood events in Niamey. *Atmos Res*. <https://doi.org/10.1016/j.atmosres.2015.01.010>
- Casse C, Gosset M, Vischel T, Quantin G, Tanimoun BA (2016) Model-based study of the role of rainfall and land use-land cover in the changes in the occurrence and intensity of Niger red floods in Niamey between 1953 and 2012. *Hydrol Earth Syst Sci*. <https://doi.org/10.5194/hess-20-2841-2016>
- Chini M, Pelich R, Pulvirenti L, Pierdicca N, Hostache R, Matgen P (2019) Sentinel-1 InSAR coherence to detect floodwater in urban areas: Houston and hurricane Harvey as a test case. *Remote Sens* 11:107. <https://doi.org/10.3390/rs11020107>
- Cooper ES, Dance SL, García-Pintado J, Nichols NK, Smith PJ (2019) Observation operators for assimilation of satellite observations in fluvial inundation forecasting. *Hydrol Earth Syst Sci* 23(6):2541–2559. <https://doi.org/10.5194/hess-23-2541-2019>
- CRED (2020) Human cost of disasters, an overview of the last 20 years (2000–2019)
- Dasgupta A, Hostache R, Ramsankaran RAAJ, Schumann GJ-P, Grimaldi S, Pauwels V, Walker J (2021a) A mutual information-based likelihood function for particle filter flood extent assimilation. *Water Resour Res* 52(2):e2020WR027859. <https://doi.org/10.1029/2020WR027859>
- Dasgupta A, Hostache R, Ramsankaran RAAJ, Schumann GJ-P, Grimaldi S, Pauwels V, Walker J (2021b) On the impacts of observation location, timing and frequency on flood extent assimilation performance. *Water Resour Res* 52(2):e2020WR028238. <https://doi.org/10.1029/2020WR028238>
- Di Baldassarre G, Montanari A, Lins H, Koutsoyiannis D, Brandimarte L, Blöschl G (2010) Flood fatalities in Africa: from diagnosis to mitigation. *Geophys Res Lett*. <https://doi.org/10.1029/2010GL045467>
- Di Mauro C, Hostache R, Matgen P, Pelich R, Chini M, van Leeuwen PJ, Nichols N, Blöschl G (2021) Assimilation of probabilistic flood maps from SAR data into a hydrologic-hydraulic forecasting model: a proof of concept. *Hydrol Earth Syst Sci* 25:4081–4097. <https://doi.org/10.5194/hess-25-4081-2021>
- Di Mauro C, Hostache R, Matgen P, Pelich R, Chini M, van Leeuwen PJ et al (2022) A tempered particle filter to enhance the assimilation of SAR-derived flood extent maps into flood forecasting models. *Water Resour Res* 58:e2022WR031940. <https://doi.org/10.1029/2022WR031940>
- Fiolleau T, Roca R (2013) An algorithm for the detection and tracking of tropical mesoscale convective systems using infrared images from geostationary satellite. *IEEE Trans Geosci Remote Sens* 51:4302–4315. <https://doi.org/10.1109/TGRS.2012.2227762>
- Fleischmann A et al (2018) Modelling hydrologic and hydrodynamic processes in basins with large semi-arid wetlands. *J Hydrol* 561:943–959. <https://doi.org/10.1016/j.jhydrol.2018.04.041>
- Floodlist (2019) www.floodlist.com
- Giorgi F, Im E-S, Coppola E, Diffenbaugh NS, Gao XJ, Mariotti L, Shi Y (2011) Higher hydroclimatic intensity with global warming. *J Clim* 24:5309–5324. <https://doi.org/10.1175/2011JCLI3979.1>
- Giustarini L et al (2016) Probabilistic flood mapping using synthetic aperture radar data. *IEEE Trans Geosci Remote Sens* 54(12):6958–6969. <https://doi.org/10.1109/TGRS.2016.2592951>
- Gosset M et al (2016) Improving rainfall measurement in gauge poor regions thanks to mobile telecommunication networks. *Bull Am Meteorol Soc*. <https://doi.org/10.1175/BAMS-D-15-00164.1>
- Gosset M, Alcoba M, Roca R, Cloché S, Urbani G (2018) Evaluation of TAPEER daily estimates and other GPM-era products against dense gauge networks in West Africa, analysing ground reference uncertainty. *Q J R Meteorol Soc* 144:255–269. <https://doi.org/10.1002/qj.3335>
- Guilloteau C, Roca R, Gosset M, Laboratoire OCA, Iii T, Toulouse E, Iii T (2016) A multiscale evaluation of the detection capabilities of high-resolution satellite precipitation products in West Africa. *J Hydrometeorol*. <https://doi.org/10.1175/JHM-D-15-0148.1>
- Guilloteau C, Foufoula-Georgiou E, Kirstetter P, Tan J, Huffman GJ (2021) How well do multisatellite products capture the space-time dynamics of precipitation? Part I: Five products assessed via a wavenumber-frequency decomposition. *J Hydrometeorol* 22:2805–2823. <https://doi.org/10.1175/JHM-D-21-0075.1>

- Haile AT, Asfaw W, Rientjes T, Worako AW (2022) Deterioration of streamflow monitoring in Omo-Gibe basin in Ethiopia. *Hydrol Sci J*. <https://doi.org/10.1080/02626667.2022.2060110>
- Hall AC, Schumann GJ-P, Bamber JL, Bates PD, Trigg MA (2012) Geodetic corrections to Amazon River water level gauges using ICESat altimetry. *Water Resour Res*. <https://doi.org/10.1029/2011WR010895>
- Hawley K, Moench M, Sabbag L (2012) Understanding the economics of flood risk reduction: a preliminary analysis—understanding the economics of flood risk reduction: a preliminary analysis. *isett.*, <https://www.i-s-e-l.org/publications-and-resources-1/understanding-the-economics-of-flood-risk-reduction%3A-a-preliminary-analysis>. Accessed 7 Oct 2022
- Hostache R, Matgen P, Schumann G, Puech C, Hoffmann L, Pfister L (2009) Water level estimation and reduction of hydraulic model calibration uncertainties using satellite SAR images of floods. *IEEE Trans Geosci Remote Sens* 47(2):431–441. <https://doi.org/10.1109/TGRS.2008.2008718>
- Hostache R, Lai X, Monnier J, Puech C (2010) Assimilation of spatially distributed water levels into a shallow-water flood model. Part II: Use of a remote sensing image of Mosel river. *J Hydrol* 390(3–4):257–268. <https://doi.org/10.1016/j.jhydrol.2010.07.003>
- Hostache R, Chini M, Giustarini L, Neal J, Kavetski D, Wood M, Corato G, Pelich RM, Matgen P (2018) Near-real-time assimilation of SAR derived flood maps for improving flood forecasts. *Water Resour Res* 54(8):5516–5535. <https://doi.org/10.1029/2017WR022205>
- Huffman GJ et al (2020) Integrated multi-satellite retrievals for the global precipitation measurement (GPM) Mission (IMERG). Satellite precipitation measurement: Volume 1. In: Levizzani V, Kidd C, Kirschbaum DB, Kummerow CD, Nakamura K, Turk FJ (eds) *Advances in Global Change Research*. Springer International Publishing, Cham, pp 343–353
- IPCC (2022) *Climate Change 2022: impacts, adaptation, and vulnerability*. contribution of working group II to the sixth assessment report of the intergovernmental panel on climate change. In: Pörtner H-O, Roberts DC, Tignor M, Poloczanska ES, Mintenbeck K, Alegría A, Craig M, Langsdorf S, Lösschke S, Möller V, Okem A, Rama B (eds). Cambridge University Press, Cambridge University Press, Cambridge, New York, NY, p 3056. <https://doi.org/10.1017/9781009325844>.
- Kidd C, Levizzani V (2011) Status of satellite precipitation retrievals. *Hydrol Earth Syst Sci* 15:1109–1116. <https://doi.org/10.5194/hess-15-1109-2011>
- Kidd C, Becker A, Huffman GJ, Muller CL, Joe P, Skofronick-Jackson G, Kirschbaum DB (2017) So, How much of the earth's surface is covered by rain gauges? *Bull Am Meteorol Soc*. <https://doi.org/10.1175/BAMS-D-14-00283.1>
- Kidd G, Huffman V, Maggioni PC, Oki R (2021) The global satellite precipitation constellation: current status and future requirements. *Bull Am Meteorol Soc* 102:E1844–E1861. <https://doi.org/10.1175/BAMS-D-20-0299.1>
- Kitambo B et al (2021) A combined use of in situ and satellite-derived observations to characterize surface hydrology and its variability in the Congo River Basin. *Hydrol Earth Syst Sci Discuss*. <https://doi.org/10.5194/hess-2021-315>
- Kubota T et al. (2020) Global Satellite mapping of precipitation (GSMaP) products in the GPM era. Satellite precipitation measurement: Volume 1, In: Levizzani V, Kidd C, Kirschbaum DB, Kummerow CD, Nakamura K, Turk FJ (eds), *Advances in Global Change Research*, Springer International Publishing, Cham, pp 355–373
- Kummerow CD (2020) Introduction to passive microwave retrieval methods. In: Levizzani V, Kidd C, Kirschbaum DB, Kummerow CD, Nakamura K, Turk FJ (eds) *Satellite Precipitation Measurement*. Springer Nature, Berlin, Heidelberg, pp 123–140
- Lai X, Liang Q, Yesou H, Daillet S (2014) Variational assimilation of remotely sensed flood extents using a 2-D flood model. *Hydrol Earth Syst Sci* 18:4325–4339. <https://doi.org/10.5194/hess-18-4325-2014>
- Landuyt L, Van Wesemael A, Schumann GJ-P, Hostache R, Verhoest NEC, Van Coillie FMB (2019) Flood mapping based on synthetic aperture radar: an assessment of established approaches. *IEEE Trans Geosci Remote Sens* 57(2):722–739. <https://doi.org/10.1109/TGRS.2018.2860054>
- Li C, Chai Y, Yang L, Li H (2016) Spatio-temporal distribution of flood disasters and analysis of influencing factors in Africa. *Nat Hazards* 82:721–731. <https://doi.org/10.1007/s11069-016-2181-8>
- Lorenz C, Kunstmann H (2012) The hydrological cycle in three state-of-the-art reanalyses: intercomparison and performance analysis. *J Hydrometeorol* 13:1397–1420. <https://doi.org/10.1175/JHM-D-11-088.1>
- Malou et al (2021) Generation and analysis of stage-fall-discharge laws from coupled hydrological-hydraulic river network model integrating sparse multi-satellite data. *J Hydrol* 603 Part C. <https://doi.org/10.1016/j.jhydrol.2021.126993>
- Martinis S, Twele A, Kersten J (2015) A fully automated TerraSAR-X based flood service. *ISPRS J Photogramm Remote Sens* 104:203–212. <https://doi.org/10.1016/j.isprsjprs.2014.07.014>

- Mason DC, Giustarini L, Garcia-Pintado J, Cloke HL (2014) Detection of flooded urban areas in high resolution synthetic aperture radar images using double scattering. *Int J Appl Earth Obs Geoinf* 28(2014):150–159. <https://doi.org/10.1016/j.jag.2013.12.002>
- Massazza G et al (2021) Recent changes in hydroclimatic patterns over medium Niger river basins at the origin of the 2020 flood in Niamey (Niger). *Water* 13:1659. <https://doi.org/10.3390/w13121659>
- Matgen P, Martinis S, Wagner W, Freeman V, Zeil P, McCormick N (2020) Feasibility assessment of an automated, global, satellite-based flood monitoring product for the Copernicus Emergency Management Service, EUR 30073 EN. Publications Office of the European Union, Ispra. <https://doi.org/10.2760/653891,JRC119812>
- Mathon V, Laurent H (2001) Life cycle of Sahelian mesoscale convective cloud systems. *Q J R Meteorol Soc.* <https://doi.org/10.1002/qj.49712757208>
- Mathon V, Lebel T (2002) Mesoscale convective system rainfall in the Sahel. *J Appl Meteorol.* [https://doi.org/10.1175/1520-0450\(2002\)041%3c1081:MCSRIT%3e2.0.CO;2](https://doi.org/10.1175/1520-0450(2002)041%3c1081:MCSRIT%3e2.0.CO;2)
- McFeeters SK (1996) The use of the normalized difference water index (NDWI) in the delineation of open water features. *Int J Remote Sens* 17:1425–1432. <https://doi.org/10.1080/01431169608948714>
- Neal JC, Schumann GJ-P, Bates PD (2012) A sub-grid channel model for simulating river hydraulics and floodplain inundation over large and data sparse areas. *Water Resour Res.* <https://doi.org/10.1029/2012WR012514>
- Nguimalet CR, Orange D (2019) Characterization of the current hydrological drop of the Ubangui River at Bangui Central African Republic, *La Houille Blanche* 105(1):78–84. <https://doi.org/10.1051/lhb/2019010>
- OCHA (2019). <https://www.unocha.org/publication/ocha-annual-report/ocha-annual-report-2019>
- O’Loughlin FE, Neal J, Schumann GJ, Beighley RE, Bates PD (2019) A LISFLOOD-FP hydraulic model of the middle reach of the Congo. *J Hydrol.* <https://doi.org/10.1016/j.jhydrol.2019.124203>
- Panthou G et al (2018) Rainfall intensification in tropical semi-arid regions: the Sahelian case. *Environ Res Lett* 13:064013. <https://doi.org/10.1088/1748-9326/aac334>
- Papa F et al (2023) Water resources in Africa under global change: monitoring surface waters from space. *Surv Geophys.* <https://doi.org/10.1007/s10712-022-09700-9>
- Pappenberger F, Cloke HL, Parker DJ, Wetterhall F, Richardson DS, Thielen J (2015) The monetary benefit of early flood warnings in Europe. *Environ Sci Policy* 51:278–291. <https://doi.org/10.1016/j.envsci.2015.04.016>
- Paris A et al. (2020) Monitoring hydrological variables from remote sensing and modelling in the Congo River basin. <https://doi.org/10.1002/ESSOAR.10505518.1>
- Pelich R, Chini M, Hostache R, Matgen P, Pulvirenti L, Pierdicca N (2022) Mapping floods in urban areas from dual-polarization InSAR coherence data. *IEEE Geosci Remote Sens Lett* 29:1–5. <https://doi.org/10.1109/LGRS.2021.3110132>
- Pulvirenti L, Squicciarino G, Fiori E, Ferraris L, Puca S (2021) A tool for pre-operational daily mapping of floods and permanent water using sentinel-1 data. *Remote Sens* 13(7):2072–4292. <https://doi.org/10.3390/rs13071342>
- Pujol L, Garambois PA, Monnier J (2022) Multi-dimensional hydrological-hydraulic model with variational data assimilation for river networks and floodplains. *Geosci Model Dev* 15(15):6085–6113. <https://doi.org/10.5194/gmd-15-6085-2022>
- Roca R, Fiolleau T (2020) Extreme precipitation in the tropics is closely associated with long-lived convective systems. *Commun Earth Environ* 1:18. <https://doi.org/10.1038/s43247-020-00015-4>
- Rogers DP, Tsirkunov VV (2010) Costs and benefits of early warning systems. Background report for the global assessment report on disaster risk reduction. <https://documents1.worldbank.org/curated/en/609951468330279598/pdf/693580ESW0P1230aster0Risk0Reduction.pdf>. Accessed 7 Oct 2022.
- Rogers DP, Tsirkunov VV (2013) Weather and climate resilience: effective preparedness through national meteorological and hydrological services. The World Bank
- Schumann G et al (2007) High-resolution 3-D flood information from radar imagery for flood hazard management. *IEEE Trans Geosci Remote Sens* 45(6):1715–1725. <https://doi.org/10.1109/TGRS.2006.888103>
- Schumann GJ-P, Moller DK (2015) Microwave remote sensing of flood inundation, *Physics and Chemistry of the Earth, Parts A/B/C.* 83–84:84–95. <https://doi.org/10.1016/j.pce.2015.05.002>
- Schumann GJ-P, Neal JC, Voisin N, Andreadis KM, Pappenberger F, Phanthuwongpakdee N, Hall AC, Bates PD (2013) A first large scale flood inundation forecasting model. *Water Resour Res* 49:6248–6257. <https://doi.org/10.1002/wrcr.20521>
- Sherpa SF, Shirzaei M, Ojha C, Werth S, Hostache R (2020) Probabilistic mapping of August 2018 flood of Kerala, India, using space-borne synthetic aperture radar. *IEEE J Select Top Appl Earth Obs Remote Sens* 13:896–913. <https://doi.org/10.1109/JSTARS.2020.2970337>

- Tarpanelli A, Mondini AC, Camici S (2023) Effectiveness of Sentinel-1 and Sentinel-2 for flood detection assessment in Europe. *Nat Hazards Earth Syst Sci* 22:2473–2489. <https://doi.org/10.5194/nhess-22-2473-2022>
- Taylor CM et al (2017) Frequency of extreme Sahelian storms tripled since 1982 in satellite observations. *Nature* 544:475–478. <https://doi.org/10.1038/nature22069>
- Tiepolo M, Galligari A (2021) Urban expansion-flood damage nexus: evidence from the Dosso Region, Niger. *Land Use Policy* 108:105547. <https://doi.org/10.1016/j.landusepol.2021.105547>
- Tramblay et al (2021) ADHI: the African Database of Hydrometric Indices (1950–2018). *Earth Syst Sci Data* 13:1547–1560. <https://doi.org/10.5194/essd-13-1547-2021>
- Tramblay Y, Villarini G, Zhang W (2020) Observed changes in flood hazard in Africa. *Environ Res Lett* 15:1040b5. <https://doi.org/10.1088/1748-9326/abb90b>
- Turko M, Gosset M, Kacou M, Bouvier C, Chahinian N, Boone A, Alcoba M (2021) Rainfall measurement from Commercial microwave links for urban hydrology in Africa: a simulation framework for sensitivity analysis. *J Hydrometeorol*. <https://doi.org/10.1175/JHM-D-20-0163.1>
- UNISDR (2015). <https://www.undrr.org/publication/global-assessment-report-disaster-risk-reduction-2015>
- United Nation Development program (UNDP) (2004) Reducing disaster risk, a challenge for development. <https://www.undp.org/publications/reducing-disaster-risk-challenge-development>. <https://www.undp.org/sites/g/files/zskgke326/files/publications/Reducing%20Disaster%20risk%20a%20Challenge%20for%20development.pdf>
- Wongchuig-Correa S, de Paiva RCD, Biancamaria S, Collischonn W (2020) Assimilation of future SWOT-based river elevations, surface extent observations and discharge estimations into uncertain global hydrological models. *J Hydrol*. <https://doi.org/10.1016/j.jhydrol.2020.125473>
- WorldBank (2021) An EPIC response: innovative governance for Flood and Drought Risk Management. World Bank. <https://www.worldbank.org/en/topic/water/publication/an-epic-response-innovative-governance-for-flood-and-drought-risk-management>. Accessed 23 Jan 2022.
- Wright DB (2015) Methods in Flood Hazard and Risk Assessment. World Bank. <https://openknowledge.worldbank.org/handle/10986/22982>
- Zhao J, Pelich R, Hostache R, Matgen P, Cao S, Wagner W, Chini M (2021) Deriving exclusion maps from C-band SAR time-series in support of floodwater mapping. *Remote Sens Environ* 265:112668. <https://doi.org/10.1016/j.rse.2021.112668>

Publisher's Note Springer Nature remains neutral with regard to jurisdictional claims in published maps and institutional affiliations.